

A Retrieval Augmented Spatio-Temporal Framework for Traffic Prediction

Weilin Ruan¹, Xilin Dang², Ziyu Zhou¹, Sisuo Lyu¹, Yuxuan Liang^{1,†}

¹The Hong Kong University of Science and Technology (Guangzhou) ²The Chinese University of Hong Kong

[†]Corresponding Author: yuxliang@outlook.com

Abstract—Traffic prediction is a cornerstone of modern intelligent transportation systems and a critical task in spatio-temporal forecasting. Although advanced Spatio-temporal Graph Neural Networks (STGNNs) and pre-trained models have achieved significant progress in traffic prediction, two key challenges remain: (i) limited contextual capacity when modeling complex spatio-temporal dependencies, and (ii) low predictability at fine-grained spatio-temporal points due to heterogeneous patterns.

Inspired by Retrieval-Augmented Generation (RAG), we propose RAST, a universal framework that integrates retrieval-augmented mechanisms with spatio-temporal modeling to address these challenges. Our framework consists of three key designs: 1) Decoupled Encoder and Query Generator to capture decoupled spatial and temporal features and construct a fusion query via residual fusion; 2) Spatio-temporal Retrieval Store and Retrievers to maintain and retrieve vectorized fine-grained patterns; and 3) Universal Backbone Predictor that flexibly accommodates pre-trained STGNNs or simple MLP predictors. Extensive experiments on six real-world traffic networks, including large-scale datasets, demonstrate that RAST achieves superior performance while maintaining computational efficiency.

I. INTRODUCTION

Traffic prediction stands as a cornerstone of modern Intelligent Transportation Systems (ITS), enabling critical applications including traffic management, route optimization, and congestion mitigation [1], [2]. The accurate forecasting of traffic conditions directly impacts urban mobility, economic efficiency, and environmental sustainability across metropolitan areas worldwide. Spatio-temporal Forecasting (STF) provides the methodological foundation for addressing these traffic prediction challenges, as traffic data inherently exhibits complex interdependencies across both spatial and temporal dimensions [3], [4].

The evolution of STF methodologies has progressed from traditional statistical approaches [5], [6], [7] to sophisticated deep learning architectures [8], [9], [10] as application scenarios have become increasingly complex. This progression culminated in the development of Spatio-temporal Graph Neural Networks (STGNNs) [11], [12], [13], which have achieved remarkable success in modeling complex spatial-temporal dependencies by representing traffic networks as graphs and leveraging graph convolution operations [14], [15]. More recently, the emergence of Large Models (LMs) and pre-trained models from Natural Language Processing (NLP) [16], [17] and Computer Vision (CV) [18], [19] has opened new opportunities for enhancing spatio-temporal forecasting capabilities [20], [21], [22].

Despite these advances, current STF approaches face two critical limitations: (i) **Limited Contextual Capacity vs. scale**

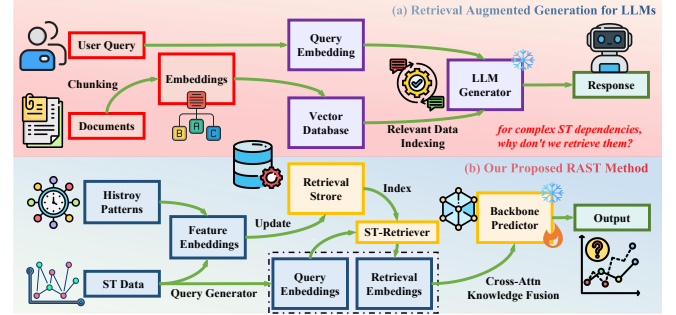


Fig. 1: Motivation of RAST. Inspired by retrieval-augmented generation for large language models, we design a specialized retrieval-augmented framework for STF tasks.

of ST data: Contemporary pre-trained STGNNs suffer from constrained contextual embedding capacity when handling complex spatio-temporal dependencies in large-scale traffic networks [23], [24], [25]. Drawing inspiration from retrieval-augmented generation (RAG) that has shown promise in addressing context limitations in Large Language Models (LLMs) [26], we investigate whether retrieval-augmented mechanisms can compensate for the limited spatio-temporal learning capacity, as illustrated in Figure 1; (ii) **Complex Architecture vs. Low Predictability:** Due to the inherent heterogeneity in spatio-temporal data [4], existing STF approaches lack efficient mechanisms for fine-grained pattern adjustment within limited embedding lengths [4], [23], [24]. Current performance improvements of the STGNNs rely heavily on complex model architectures [27], [28] to capture overall trends, yet low-predictability points in both temporal and spatial dimensions remain difficult to capture. Instead of further increasing model complexity by adding more weighted parameters, we propose to capture complex spatio-temporal dependencies through explicit memory storage and retrieval mechanisms, as demonstrated in Figure 2.

To bridge the gap in applying RAG to STF and further address the aforementioned challenges, we propose RAST (Retrieval-Augmented Spatio-Temporal forecasting), a universal framework that integrates retrieval-augmented mechanisms with spatio-temporal modeling for traffic prediction and pre-trained model enhancements. Specifically, our approach maintains a vector-based dual-dimension spatio-temporal retrieval store. During training, our method decouples input data into spatial and temporal encodings used to update the store while

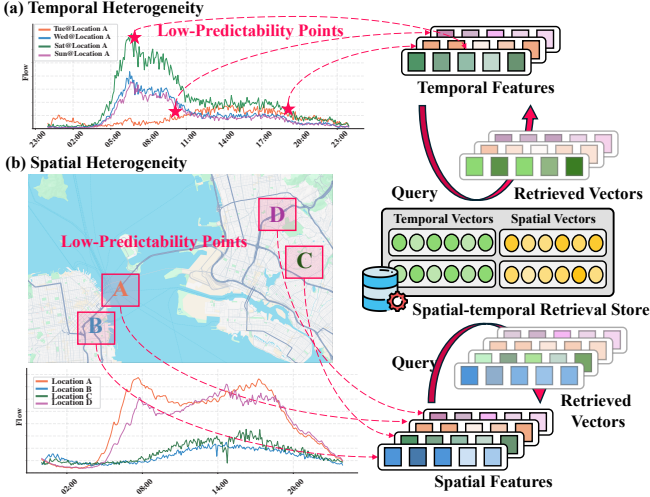


Fig. 2: The spatial and temporal heterogeneity problem (a and b). Our methods utilize a retrieval-augmented mechanism with dual-dimension vector storage. By extracting low-predictable data points and retrieving history patterns, we improve model capability in those challenging cases.

constructing context-aware queries through residual fusion. ST-Retrievers then search and project dual-dimension retrieval embeddings under queries. Finally, we fuse decoupled retrieval embeddings with current queries through a cross-attention module and obtain predictions via the universal backbone predictor. Our contributions are summarized as follows:

- **A Universal Retrieval-Augmented Framework for Spatio-temporal Forecasting:** We introduce RAST, the first retrieval-augmented framework specifically designed for spatio-temporal forecasting while providing a universal framework for existing pre-trained STGNNs as an enhancement method without expanding the model capacity.
- **A Spatio-temporal Retrieval Store and ST-Retriever for Low-Predictability Patterns:** We design a spatio-temporal retrieval store that vectorizes dual-dimension features and maintains them within memory banks, combined with optimization techniques for efficient memory and retrieval of complex spatio-temporal patterns.
- **Comprehensive Empirical Validation:** Extensive experiments on six real-world datasets demonstrate that our proposed method effectively captures complex spatio-temporal patterns while maintaining high computational efficiency, achieving up to 24.75% improvement in average MAE compared to the RPMixer on the SD dataset.

II. RELATED WORK

a) *Spatio-temporal Forecasting (STF)*: is a fundamental task in numerous application domains such as traffic management, urban planning, and environmental monitoring [29], [4], [30], [31], [32]. Early deep learning methods combined CNNs and RNNs [8], [10] but struggled with non-Euclidean traffic networks. The emergence of Spatio-temporal Graph Neural Networks (STGNNs) addressed this limitation by integrating Graph Neural Networks (GNNs) [9] with temporal models [14],

[33], [12], [13], [34], [27], [35], [11], [15], [36]. Despite these advancements, the performance improvements of STGNNs have begun to plateau due to limited contextual capacity and reliance on increasingly complex architectures [37], [23]. This stagnation has prompted research toward integrating pre-trained models and Large Language Models (LLMs) [20], [38], [21], [39], [40] to enhance predictive capabilities. *However, these methods still struggle to capture spatio-temporal heterogeneity in large-scale scenarios, while universal solutions for contextual capacity limitations in spatio-temporal modeling remain largely unexplored.*

b) *Retrieval-Augmented Generation (RAG)*: has emerged as a transformative paradigm for enhancing large language model performance, particularly in knowledge-intensive tasks [41], [26], [42]. Traditional LLMs struggle with tasks requiring vast amounts of factual knowledge or domain-specific expertise due to finite parametric memory and limited context [43], [44]. RAG addresses this limitation by integrating external retrieval mechanisms that enable models to dynamically access relevant information from large knowledge bases during inference [45], [46], [47], improving open-domain question answering, fact-checking, and few-shot learning tasks [48], [49]. *While the retrieval-augmented mechanism has been extensively studied in natural language processing, its application to vast spatio-temporal scenarios presents significant opportunities, particularly given the similar challenges of constrained model capacity.*

III. METHODOLOGY

In this section, we present **RAST**, a **Retrieval Augmented Spatio-Temporal** forecasting framework as illustrated in Figure 3.

Our approach consists of three core components working synergistically: 1) *Decoupled Encoder Layers* that convert raw inputs into vectorized embedding representations, 2) *Query Generator* that constructs fusion queries via residual fusion, 3) *Retrieval Store* that maintains and fine-grained historical patterns 4) *ST-Retriever* that retrieves embeddings based on queries and further fuses them with cross-attention blocks, and 5) *Backbone Predictor* that accommodates diverse pre-trained STGNNs or simple predictors (e.g. MLP) for enhanced forecasting performance.

A. Problem Formulation

Let $\mathcal{G} = (\mathcal{V}, \mathcal{E}, \mathcal{A})$ denote a spatio-temporal graph where $\mathcal{V} = \{v_1, v_2, \dots, v_N\}$ represents the set of N spatial nodes. \mathcal{E} represents the edges connecting spatially related nodes, and $\mathcal{A} \in \mathbb{R}^{N \times N}$ is the adjacency matrix encoding spatial relationships. At each time step t , we observe a D_{in} feature dimension matrix $X_t \in \mathbb{R}^{N \times D_{in}}$ at time t . Given historical observations $\mathbf{X} = \{X_{t-L+1}, X_{t-L+2}, \dots, X_t\} \in \mathbb{R}^{L \times N \times D_{in}}$ over L time steps, the spatio-temporal forecasting task aims to predict future observations $\mathbf{Y} \in \mathbb{R}^{H \times N \times D_{out}}$ over the next H horizons. The external memory bank \mathcal{M} is introduced and dynamically updated in our approach. Formally, we seek to learn a mapping function with the retrieval-augmented mechanism:

$$f_\theta : \mathbf{X} \times \mathcal{G} \times \mathcal{M} \rightarrow \mathcal{Y} \quad (1)$$

where θ represents the learnable parameters of the model.

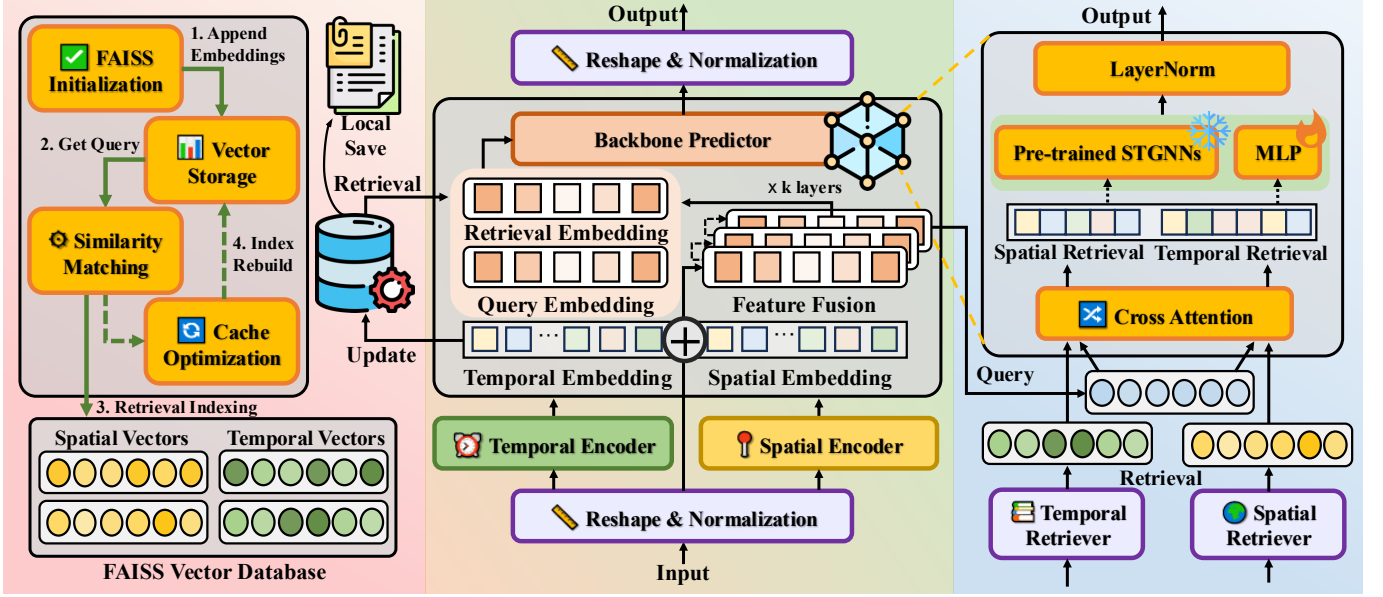


Fig. 3: Overview of the RAST framework. RAST integrates retrieval mechanisms with spatio-temporal modeling to enhance performance by maintaining and utilizing historical patterns. The proposed approach addresses the fundamental challenge of capturing long-term dependencies and complex spatio-temporal correlations in time series data.

B. Data Encoding and Query Construction

a) Dual-dimension Feature Disentanglement.: Following recent advances in spatio-temporal modeling [50], we employ decoupled encoder layers to separately process temporal and spatial information. This encoding module initially captures basic characteristics (e.g., cyclicity for temporal, regionality for spatial) formulated as follows:

$$\mathbf{E}_{tp} = \sigma(\text{Conv2D}(\mathbf{X})) \in \mathbb{R}^{B \times N \times D_{tp}} \quad (2)$$

$$\mathbf{E}_{sp} = \sigma(\mathbf{W}_{sp}(\mathbf{X}, \mathcal{G})) \in \mathbb{R}^{B \times N \times D_{sp}} \quad (3)$$

where $\sigma(\cdot)$ denotes the reshape and normalization operation for the corresponding dimension. D_{tp}, D_{sp} are temporal and spatial feature dimension. The 2D convolutional kernel is initialized using Kaiming normal initialization to ensure stable training dynamics, while the spatial transformation matrix \mathbf{W}_{sp} is initialized with Xavier uniform distribution.

b) Context-Aware Query Generation.: To construct an input that retrieves the most similar embedding, we designed a specific query generator. Specifically, the temporal and spatial embeddings are concatenated and projected to a fusion representation $\mathbf{E}_f^{(0)}$. Then we construct context-aware query representations \mathbf{Q}_{st} through L encoder layers with residual connections as follows:

$$\mathbf{E}_f^{(0)} = \text{Linear}_Q(\text{Concat}[\mathbf{E}_{sp}; \mathbf{E}_{tp}]), \quad (4)$$

$$\mathbf{E}_f^{(l+1)} = \text{LayerNorm}(\mathbf{E}_f^{(l)} + \text{FFN}(\mathbf{E}_f^{(l)})), \quad (5)$$

$$\mathbf{Q}_{st} = \mathbf{E}_f^{(L)} \in \mathbb{R}^{B \times N \times D_q} \quad (6)$$

where FFN denotes a feed-forward network with ReLU activation and dropout for regularization.

C. Spatio-temporal Retrieval Store

a) Pattern Indexing and Storage.: Traditional spatio-temporal models suffer from limited contextual capacity when handling complex dependencies, while we introduce a dual-dimension memory bank $\mathcal{M} = \{\mathcal{M}_{sp}, \mathcal{M}_{tp}\}$ that dynamically maintains vectorized historical patterns:

$$\mathcal{M}_{sp} = \{\mathbf{v}_{sp}^{(i)}, \mathbf{m}_{sp}^{(i)}\}_{i=1}^{|\mathcal{M}_{sp}|}, \mathcal{M}_{tp} = \{\mathbf{v}_{tp}^{(j)}, \mathbf{m}_{tp}^{(j)}\}_{j=1}^{|\mathcal{M}_{tp}|} \quad (7)$$

where $\mathbf{v}^{(i)}, \mathbf{v}^{(j)}$ represent chunked embedding vectors and $\mathbf{m}^{(i)}, \mathbf{m}^{(j)}$ contain associated metadata including statistical summaries and importance measures for sustainable storage.

To enable fast similarity search, our retrieval store utilizes the Facebook AI Similarity Search (FAISS) library [51], [52] for efficient similarity-based indexing. Given history queries \mathbf{Q}_{st} and current state e , we maintain and compute indices \mathcal{I} for temporal and spatial embeddings (more details in Appendix D):

$$\mathcal{I}_{sp} = \sigma(\text{Index}(\{\mathbf{v}_{sp}^{(e)}\} \in \mathcal{M}_{sp} | \mathbf{Q}_{st})) \quad (8)$$

$$\mathcal{I}_{tp} = \sigma(\text{Index}(\{\mathbf{v}_{tp}^{(e)}\} \in \mathcal{M}_{tp} | \mathbf{Q}_{st})) \quad (9)$$

where $\mathbf{v}_s^{(e)}, \mathbf{v}_t^{(e)}$ represent the sampled decoupled vectors and $\sigma(\cdot)$ denotes the operation of discretization. The indices support (i) periodic rebuild, (ii) LRU caching, and (iii) GPU Acceleration, significantly improving retrieval efficiency.

1) Information-Theoretic ST-Retriever.: To identify and select the most relevant historical patterns of vectors from the retrieval store, we defined spatio-temporal retrievers to search for the Top-k most relevant information based on the similarity searching function $\text{Retriever}(\cdot)$. Given a context-aware query $\mathbf{Q} \in \mathbb{R}^{B \times N \times D_q}$ and the computed indices \mathcal{I} , the retriever performs fine-grained pattern discovery utilizing L2 distance as follows:

$$\mathcal{D}(\mathbf{Q}, \mathbf{v}_i) = -\|\mathbf{Q} - \mathbf{v}_i\|_2^2 \quad (10)$$

$$\text{Retriever}(\mathcal{Q}, \mathcal{I}, k) = \arg \max_k \{\mathcal{D}(\mathcal{Q}, \mathbf{v}_j)\}_{j=1}^{|\mathcal{V}|} \quad (11)$$

where \mathbf{v} represents chunked pattern vectors in the memory bank \mathcal{M} indexing by $\mathcal{M}(\mathcal{I}) \mapsto \mathcal{V}$.

Given dual-dimension feature $\mathbf{E}_{sp}, \mathbf{E}_{tp}$ encoded before, the set of indices \mathcal{I} of lengths k , the ST-retrievers match the fine-grained pattern sets in the retrieval store and calculate the momentum of the memory banks as follows:

$$\mathcal{E}_s = \text{Retriever}(\mathbf{E}_{sp}, \mathcal{I}_s, k) = \{(\mathbf{v}_s^{(i)}, \omega_s^{(i)})\}_{i=1}^k \quad (12)$$

$$\mathcal{E}_t = \text{Retriever}(\mathbf{E}_{tp}, \mathcal{I}_t, k) = \{(\mathbf{v}_t^{(j)}, \omega_t^{(j)})\}_{j=1}^k \quad (13)$$

To enhance the quality of retrieved vectors $\mathbf{v}_i \in \{\mathcal{E}_s, \mathcal{E}_t\}$, we incorporate the similarity score $s_i = \mathcal{D}(\mathcal{Q}, \mathbf{v}_i)$ and momentum scores ω_i that enable weighted pattern aggregation. Given information entropy function $\mathcal{H}(\mathbf{v}) = -\sum_{d=1}^D p_d \log p_d$ where $p_d = \frac{\exp(\mathbf{v}_d)}{\sum_{j=1}^D \exp(\mathbf{v}_j)}$ measures the information entropy, the momentum scores are updated with the diversity-similarity coefficient λ and the temperature parameter τ for confidence calibration as follows:

$$\omega'_i = \omega_i + \text{softmax}(s_i + \lambda \cdot \mathcal{H}(\mathbf{v}_i)) / \tau \quad (14)$$

2) *Momentum-Based Memory Management*: The retrieval store is updated periodically during training with a defined interval to balance between pattern freshness and computational overhead. To prevent unbounded memory growth while preserving both recent and historically significant patterns, we implement adaptive memory management:

$$\mathcal{M}_s^{(e+1)} = (1 - \omega^s) \mathcal{M}_s^{(e)} + \omega_s \cdot \sigma(\mathcal{E}_s) \quad (15)$$

$$\mathcal{M}_t^{(e+1)} = (1 - \omega^t) \mathcal{M}_t^{(e)} + \omega_t \cdot \sigma(\mathcal{E}_t) \quad (16)$$

where $\sigma(\cdot)$ denotes an insertion, and adaptive memory parameters α, β are determined by similarity scores s , ensuring optimal balance between memory freshness and stability.

a) *Cross-Attention Knowledge Fusion*: Rather than simply taking the retrieval vectors separated by temporal and spatial dimensions, we employ multi-head attention mechanisms to further fuse query embeddings with retrieved patterns:

$$\text{Attn}(\mathbf{Q}, \mathbf{K}, \mathbf{V}) = \text{softmax}\left(\frac{\mathbf{Q}\mathbf{K}^\top}{\sqrt{d_k}}\right) \mathbf{V} \quad (17)$$

$$\mathcal{R}_t = \text{Attn}(\mathcal{Q}_{st}, \mathcal{E}_t, \mathcal{E}_t), \quad \mathcal{R}_s = \text{Attn}(\mathcal{Q}_{st}, \mathcal{E}_s, \mathcal{E}_s) \quad (18)$$

$$\mathcal{R}_f = \text{Attn}(\mathcal{Q}_{st}, \mathcal{R}_s, \mathcal{R}_t), \quad \mathbf{H}_f = \text{Concat}[\mathcal{Q}_{st}; \mathcal{R}_f] \quad (19)$$

where $\mathcal{R}_f \in \mathbb{R}^{B \times N \times D_r}$ denotes the fused retrieval with embedding dimension D_r and \mathbf{H}_f is the fusion embedding that preserves the original query while combining with the most relevant dual-dimension retrieved patterns.

D. Prediction and Optimization

a) *Universal Backbone Predictor*: For prediction generation, we utilized function $\mathcal{B}(\mathbf{X}, \mathbf{H}_f, \mathcal{G}) \mapsto \mathcal{Y}$, leveraging a universal backbone network $\mathcal{B}(\cdot)$ for fine-tuning tasks or training from scratch. We designed a universal interface that allows frozen or learnable pre-trained STGNNs to use our retrieval-augmented mechanisms, accommodating various backbone configurations without modification to the core

retrieval mechanism for improvements. And for the following experiments, we default to applying the lightweight Multilayer Perceptron (MLP) as \mathcal{B} in the fair perspective.

b) *Prediction Generation*: We employ a residual enhancement pipeline preserving information flow while enabling architectural flexibility, with layer normalization and feed-forward operation after. The combined feature representation $\mathbf{Z} \in \mathbb{R}^{B \times N \times (D_q + D_r)}$ is processed through the backbone predictor to generate final predictions:

$$\mathbf{Z} = \mathcal{B}(\mathbf{H}_f) \parallel \text{Conv}(\sigma(\text{Conv}(\mathbf{H}_f \cdot \mathbf{W}_1 + b_1))\mathbf{W}_2 + b_2) \quad (20)$$

$$\hat{\mathcal{Y}} = \text{LayerNorm}(\mathbf{Z}) + \text{FFN}(\mathbf{Z}) \quad (21)$$

c) *Loss Function*: The model is trained using Mean Absolute Error (MAE) loss with L2 regularization:

$$\mathcal{L} = \frac{1}{M} \sum_{i \in M} \|\hat{\mathcal{Y}}_i - \mathcal{Y}_i\| + \lambda \|\theta\|^2 \quad (22)$$

where λ is the regularization coefficient for model parameter θ , and M denotes the collection of valid data points.

IV. EXPERIMENTS

We conduct extensive experiments to evaluate the effectiveness of RAST in multiple ways. These experiments are designed to answer the following Research Questions (RQ):

- **RQ1**: How does RAST perform compared to state-of-the-art spatio-temporal forecasting methods?
- **RQ2**: What is the individual contribution of each component in the RAST framework?
- **RQ3**: How sensitive is RAST to key hyperparameters?
- **RQ4**: What is the computational efficiency of RAST compared to baseline methods?

A. Experimental Settings

a) *Datasets and Baselines*: We conducted comprehensive experiments across six diverse traffic networks: 1) PEMS03, PEMS04, PEMS07, PEMS08 [53] datasets, and 2) the large-scale dataset San Diego (SD), Greater Bay Area (GBA) as introduced in LargeST [25]. Detailed statistics of these datasets are shown in Table II. We compare our RAST with 21 classic or advanced baselines, which are categorized into 3 groups: (i) **Non-spatial methods**: ARIMA [5]VAR [6], SVR [54], LSTM [10], TCN [55], Transformer [56]; (ii) **GNN-based Spatial-temporal Models** DCRNN [14], STGCN [12], ASTGCN [34], GWNet [15], LSGCN [57], STSGCN [53], STFGNN [58], STCODE [59], DSTAGNN [28], AGCRN [13], D2STGNN [27] and (iii) **Other Enhanced Approaches**: Z-GCNETs [60], TAMP [61], STKD [62], RPMixer [63]. More details of the baselines are given in Appendix A.

b) *Metrics and Settings*: Performance is evaluated using standard metrics, including MAE, RMSE, and MAPE. We use 12 historical time steps to forecast the next 12 steps and calculate the average across horizons 3, 6, and 12. For the fairness of the experiment, we only utilized the simple MLP trained from scratch as the backbone predictor in the following experiments. All models are implemented in PyTorch and trained on Nvidia RTX A6000 GPUs with consistent

Methods	PEMS03			PEMS04			PEMS07			PEMS08		
	MAE	RMSE	MAPE(%)	MAE	RMSE	MAPE(%)	MAE	RMSE	MAPE(%)	MAE	RMSE	MAPE(%)
ARIMA	35.31	47.59	33.78	33.73	48.80	24.18	38.17	59.27	19.46	31.09	44.32	22.73
VAR	23.65	38.26	24.51	23.75	36.66	18.09	75.63	115.24	32.22	23.46	36.33	15.42
SVR	21.97	35.29	21.51	28.70	44.56	19.20	32.49	50.22	14.26	23.25	36.16	14.64
LSTM	21.33	35.11	23.33	27.14	41.59	18.20	29.98	45.84	13.20	22.20	34.06	14.20
TCN	19.31	33.24	19.86	31.11	37.25	15.48	32.68	42.23	14.22	22.69	35.79	14.04
Transformer	17.50	30.24	16.80	23.83	37.19	15.57	26.80	42.95	12.11	18.52	28.68	13.66
DCRNN	18.18	30.31	18.91	24.70	38.12	17.12	25.30	38.58	11.66	17.86	27.83	11.45
STGCN	17.49	30.12	17.15	22.70	35.55	14.59	25.38	38.78	11.08	18.02	27.83	11.40
ASTGCN	17.69	29.66	19.40	22.93	35.22	16.56	28.05	42.57	13.92	18.61	28.16	13.08
GWNet	19.85	32.94	19.31	25.45	39.70	17.29	26.85	42.78	12.12	19.13	31.05	12.68
LSGCN	17.94	29.85	16.98	21.53	33.86	13.18	27.31	41.16	11.98	17.73	26.76	11.30
STSGCN	17.48	29.21	16.78	21.19	33.65	13.90	24.26	39.03	10.21	17.13	26.80	10.96
STFGNN	16.77	28.34	16.30	19.83	31.88	13.02	22.07	35.80	9.21	16.64	26.22	10.60
STGODE	16.50	27.84	16.69	20.84	32.82	13.77	22.99	37.54	10.14	16.81	25.97	10.62
DSTAGNN	15.57	27.21	14.68	<u>19.30</u>	<u>31.46</u>	12.70	<u>21.42</u>	<u>34.51</u>	9.01	<u>15.67</u>	<u>24.77</u>	<u>9.94</u>
EnhanceNet	16.05	28.33	15.83	20.44	32.37	13.58	21.87	35.57	9.13	16.33	25.46	10.39
AGCRN	16.06	28.49	15.85	19.83	32.26	12.97	21.29	35.12	<u>8.97</u>	15.95	25.22	10.09
Z-GCNETs	16.64	28.15	16.39	19.50	31.61	<u>12.78</u>	21.77	35.17	9.25	15.76	25.11	10.01
TAMP	16.46	28.44	<u>15.37</u>	19.74	31.74	13.22	21.84	35.42	9.24	16.36	25.98	10.15
STKD	16.03	<u>25.95</u>	15.76	19.86	31.93	13.18	21.64	34.96	9.03	15.81	25.07	10.02
RAST (Ours)	15.36	25.81	16.47	18.39	29.93	12.43	19.52	32.73	8.23	14.20	23.49	9.29

TABLE I: Performance comparison assessed by averaging over all 12 prediction steps with baseline models on the PEMS03, 04, 07, 08 datasets. **Bold**: best; Underline: second best.

hyperparameter tuning protocols to ensure fair comparison. The models are trained using the Adam optimizer with a learning rate of 0.002, a batch size of 32, and a maximum of 300 epochs, applying an early stopping strategy. More detailed experimental settings are provided in Appendix B.

Datasets	#Points	#Samples	#TimeSlices	Timespan
PEMS03	358	9.38M	26,208	09/01/2018-11/30/2018
PEMS04	307	5.22M	16,992	01/01/2018-02/28/2018
PEMS07	883	24.92M	28,224	05/01/2017-08/31/2017
PEMS08	170	3.04M	17,856	07/01/2016-08/31/2016
SD	716	25M	35040	01/01/2019-12/31/2019
GBA	2352	82M	35040	01/01/2019-12/31/2019

TABLE II: The Statistics Details of the Dataset.

B. Performance Evaluation (RQ1)

Table I presents a comprehensive comparison of various approaches for traffic forecasting tasks across PEMS datasets. While the results on PEMS03 show room for improvement, RAST consistently outperforms state-of-the-art baseline methods on the remaining datasets. On the PEMS07 dataset, RAST achieves a MAE of 19.52, surpassing the second-best method DSTAGNN by 8.87%. On the PEMS08 dataset, RAST reduces RMSE by 1.58 compared to competitive STKD, while on the PEMS04, it outperforms all baselines with an MAE of 18.39 and RMSE of 29.93.

Table III extends our evaluation to larger datasets, while the performance on the horizon 3, horizon 6, horizon 12, and the average of the whole 12 horizons are reported. Our method maintains its advantage on larger traffic networks, achieving the best results at each horizon. On the SD dataset, RAST achieves an average MAE of 19.00, RMSE of 32.64, and MAPE of 12.53%, representing improvements compared to the second-best method STGODE. For the long-term prediction (Horizon

12), our method achieves the best MAE of 23.20 and RMSE of 40.72, highlighting its robustness in modeling complex long-range dependencies. On even larger traffic datasets GBA, RAST still surpasses baselines across all metrics and horizons, outperforming strong baselines like DSTAGNN and RPMixer. These results demonstrate the scalability of RAST to model complex spatio-temporal dependencies in large-scale traffic networks.

C. Ablation Study (RQ2)

We conducted comprehensive ablation studies to evaluate the contribution of each component within our RAST, with results presented in Table IV. The results demonstrate the significance of each component, with performance degradations across different metrics when components are removed or modified. The query generator emerges as the most critical component, with its removal causing the most substantial performance degradation of 25.6% in MAE, 15.4% in RMSE, and 42.9% in MAPE. This dramatic decline validates our design of context-aware query generation as fundamental to the framework’s effectiveness. Both spatial and temporal encoders prove indispensable, with their removal resulting in 17.2% and 21.2% MAE degradation respectively, confirming that dual-stream encoding effectively captures essential spatio-temporal dependencies.

Notably, the variant using only retrieval embeddings achieves superior MAE (19.38) and RMSE (30.88) compared to the full model while showing significant MAPE degradation (61.8%). This suggests that while retrieval alone captures overall magnitude, it may miss crucial distributional details, highlighting the importance of cross-attention-based fusion for balanced performance. The complete removal of the ST-retriever causes moderate degradation (11.2% of MAE, and 22.0% of MAPE), while the MLP predictor contributes significantly with 11.0%

Dataset	Methods	Horizon 3			Horizon 6			Horizon 12			Average		
		MAE	RMSE	MAPE (%)	MAE	RMSE	MAPE (%)	MAE	RMSE	MAPE (%)	MAE	RMSE	MAPE (%)
SD	LSTM	19.03	30.53	11.81	25.84	40.87	16.44	37.63	59.07	25.45	26.44	41.73	17.20
	DCRNN	<u>17.14</u>	<u>27.47</u>	11.12	20.99	<u>33.29</u>	13.95	26.99	42.86	18.67	21.03	<u>33.37</u>	14.13
	STGCN	17.45	29.99	12.42	<u>19.55</u>	33.69	13.68	<u>23.21</u>	41.23	<u>16.32</u>	19.67	34.14	13.86
	ASTGCN	19.56	31.33	12.18	24.13	37.95	15.38	30.96	49.17	21.98	23.70	37.63	15.65
	STGOE	16.75	28.04	11.00	19.71	33.56	<u>13.16</u>	23.67	42.12	16.58	<u>19.55</u>	33.57	<u>13.22</u>
	DSTAGNN	18.13	28.96	11.38	21.71	34.44	13.93	27.51	43.95	19.34	21.82	34.68	14.40
	D2STGNN	17.54	28.94	12.12	20.92	33.92	14.89	25.48	<u>40.99</u>	19.83	20.71	33.65	15.04
	RPMixer	18.54	30.33	11.81	24.55	40.04	16.51	35.90	58.31	27.67	25.25	42.56	17.64
	RAST (Ours)	16.23	26.75	10.23	19.12	32.05	12.45	23.20	40.72	16.06	19.00	32.64	12.53
GBA	LSTM	20.38	33.34	15.47	27.56	43.57	23.52	39.03	60.59	37.48	27.96	44.21	24.48
	DCRNN	18.71	30.36	<u>14.72</u>	<u>23.06</u>	<u>36.16</u>	20.45	29.85	46.06	29.93	<u>23.13</u>	<u>36.35</u>	20.84
	STGCN	21.05	34.51	16.42	23.63	38.92	<u>18.35</u>	<u>26.87</u>	<u>44.45</u>	<u>21.92</u>	23.42	38.57	<u>18.46</u>
	ASTGCN	21.46	33.86	17.24	26.96	41.38	<u>24.22</u>	<u>34.29</u>	<u>52.44</u>	32.53	26.47	40.99	23.65
	DSTAGN	19.73	31.39	15.42	24.21	37.70	20.99	30.12	46.40	28.16	23.82	37.29	20.16
	RPMixer	20.31	33.34	15.64	26.95	44.02	22.75	39.66	66.44	37.35	27.77	47.72	23.87
	RAST (Ours)	18.57	30.12	14.60	22.12	35.54	18.06	26.31	43.14	21.75	21.75	35.82	17.90

TABLE III: Large-scale traffic forecasting performance comparison of our RAST and baselines on the SD and GBA datasets. Our RAST achieves the best performance across all prediction horizons and metrics. **Bold**: best; Underline: second best.

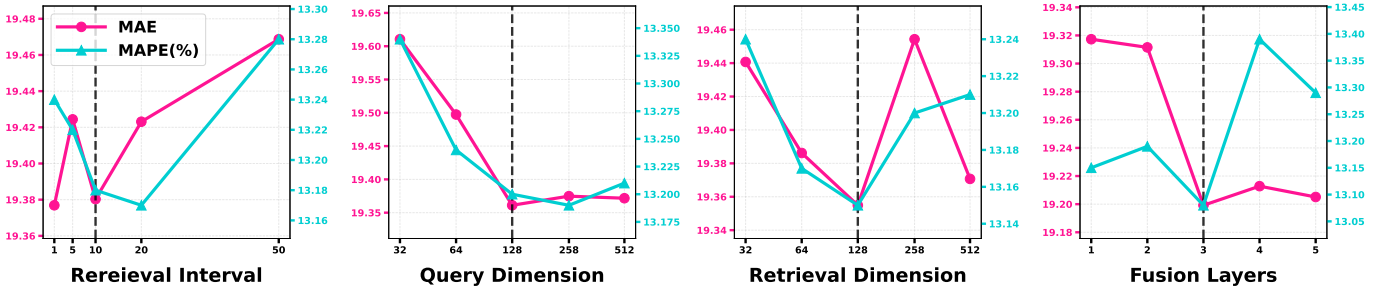


Fig. 4: Hyperparameter sensitivity analysis for RAST on the PEMS04 dataset. We chose 4 crucial hyperparameters and measured results by MAE and MAPE(%). Vertical dashed lines indicate optimal values for each parameter.

Method	MAE	RMSE	MAPE (%)
RAST (Full)	19.52	32.73	8.23
w/o Fusion Query	24.53 _{↓25.6%}	37.76 _{↓15.4%}	11.76 _{↓42.9%}
w/o ST-Retriever	21.71 _{↓11.2%}	34.58 _{↓5.7%}	10.04 _{↓22.0%}
w/o Spatial Encoder	22.88 _{↓17.2%}	35.93 _{↓9.8%}	10.10 _{↓22.7%}
w/o Temporal Encoder	23.66 _{↓21.2%}	36.90 _{↓12.7%}	10.87 _{↓32.1%}
only Query Embed.	23.59 _{↓20.9%}	36.81 _{↓12.5%}	10.79 _{↓31.1%}
only Retrieval Embed.	19.38 _{↑-0.7%}	30.88 _{↑-5.7%}	13.32 _{↓61.8%}
w/o MLP Predictor	21.67 _{↓11.0%}	34.60 _{↓5.7%}	9.52 _{↓15.7%}

TABLE IV: Ablation study results for different components on the PEMS07 dataset. We compare the full RAST with 7 variants. \downarrow Deg% denotes the degradation percentage.

MAE degradation when removed. These findings collectively validate that each component contributes uniquely to capturing complex spatio-temporal dependencies.

D. Parameter Sensitivity Analysis (RQ3)

In our parameter sensitivity analysis, we focus on 4 hyperparameters: 1) the interval of retrieval, 2) the feature dimension of query embedding, 3) the dimension of retrieval embedding, and 4) the number of fusion layers. The retrieval interval demonstrates optimal performance at 10 epochs, with infrequent updates (20, 50) causing degradation due to noise introduction and pattern staleness, respectively. Query embedding dimension significantly impacts effectiveness, with performance improving

dramatically from 32 to 128 dimensions, confirming the importance of sufficient representational capacity for encoding spatio-temporal patterns.

The retrieval dimension exhibits an optimal balance at 256, achieving the best MAE of 19.34, while both smaller and larger dimensions result in performance degradation. The number of fusion layers shows optimal results at 3 layers (MAE: 19.19), with additional layers providing minimal improvement while increasing computational costs. These results indicate that moderate parameter settings provide sufficient pattern representation without introducing excessive complexity or computational overhead.

The retrieval dimension demonstrates an optimal balance point at 256, while the retrieval interval is set to 10, with performance degrading at both smaller and larger values. The dimension of query embeddings significantly impacts model effectiveness, with prediction errors dramatically decreasing as resolution increases from 32 to 128, confirming the importance of the encoding processing of the raw data. The number of encoder layers shows substantial influence, with optimal performance at 3 layers (MAE: 19.19), while additional layers provide minimal improvement, suggesting that moderate network depth sufficiently extracts meaningful patterns without excessive computational costs.

These results indicate that our framework's performance gains benefit from both effective encoding of original data and

Dataset	GBA			SD		
Methods	Mem	Train	Val	Mem	Train	Val
AGCRN	16.39	619.16	67.63	5.37	120.14	12.39
D2STGNN	45.10	5392.56	830.39	38.36	1014.89	210.81
DCRNN	19.51	2654.61	350.11	9.14	333.83	57.22
DGCRN	38.71	2834.88	809.12	17.10	364.40	89.02
GWNet	11.24	1307.66	275.75	6.18	593.45	84.78
STGCN	3.40	852.57	151.46	2.16	302.95	66.50
RAST (Ours)	3.71	154.08	43.52	3.22	45.53	10.15

TABLE V: Memory and efficiency comparisons on large-scale datasets. Mem: CUDA memory (GB) used, Train: training time (seconds per epoch), Val: inference time (in seconds).

appropriate dimensionality of retrieval results, while requiring only moderate update frequency for the Retrieval Store without excessive computational overhead.

E. Efficiency Analysis (RQ4)

RAST demonstrates exceptional computational efficiency, as shown in Table V. We selected several models that demonstrated superior performance in previous experiments and evaluated them using maximum possible batch sizes (32 for SD and 16 for GBA) on a single GPU, recording three critical metrics: memory usage, training time per epoch, and inference time. While graph/attention-based models face a quadratic growing computational cost w.r.t. the number of nodes, RAST achieves the fastest training and inference speeds across both GBA and SD datasets, with training times of 154.08 and 45.53 seconds per epoch respectively, and inference times of 43.52 and 10.15 seconds. Though STGCN exhibits lower memory consumption, it requires significantly more time for both training and inference, highlighting that our model achieves better overall efficiency. Complex models like D2STGNN face severe scalability challenges on large datasets, while RAST maintains consistent performance scaling through the retrieval-augmented mechanism to capture low-predictability patterns under limited contextual capacity constraints, instead of relying on complex architectures. Through the sustainable storage and maintenance of the retrieval store, RAST maintains high performance while keeping the computational cost similar to STGCN, which verifies the effectiveness of our method under limited contextual capacity.

V. CONCLUSION

In this paper, we introduce RAST, a universal spatio-temporal forecasting framework that leverages retrieval-augmented mechanisms to address the challenges of modeling fine-grained spatio-temporal dependencies under limited context capacity. Extensive experiments on 6 real-world traffic datasets, including traffic prediction, ablation studies, hyperparameter sensitivity analysis, and the efficiency study, demonstrate that competitive performance of RAST on the spatio-temporal forecasting task while maintaining computational efficiency. These results underscore the potential of retrieval-augmented approaches to advance spatio-temporal modeling for large-scale and heterogeneous scenarios. Our future work will focus on (i) extending RAST to broader domains including climate modeling and

electricity demand forecasting, and (ii) optimizing inference efficiency across diverse pre-trained spatio-temporal graph neural networks.

REFERENCES

- [1] S. Chavhan and P. Venkataram, "Prediction based traffic management in a metropolitan area," *Journal of traffic and transportation engineering (English edition)*, vol. 7, no. 4, pp. 447–466, 2020.
- [2] Y. Zheng, L. Capra, O. Wolfson, and H. Yang, "Urban computing: concepts, methodologies, and applications," *ACM Transactions on Intelligent Systems and Technology (TIST)*, vol. 5, no. 3, pp. 1–55, 2014.
- [3] S. Wang, J. Cao, and S. Y. Philip, "Deep learning for spatio-temporal data mining: A survey," *IEEE transactions on knowledge and data engineering*, vol. 34, no. 8, pp. 3681–3700, 2020.
- [4] G. Jin, Y. Liang, Y. Fang, Z. Shao, J. Huang, J. Zhang, and Y. Zheng, "Spatio-temporal graph neural networks for predictive learning in urban computing: A survey," *IEEE Transactions on Knowledge and Data Engineering*, 2023.
- [5] G. E. Box, G. M. Jenkins, G. C. Reinsel, and G. M. Ljung, *Time series analysis: forecasting and control*. John Wiley & Sons, 2015.
- [6] H. Lütkepohl, *New introduction to multiple time series analysis*. Springer Science & Business Media, 2005.
- [7] S. R. Chandra and H. Al-Deek, "Predictions of freeway traffic speeds and volumes using vector autoregressive models," *Journal of Intelligent Transportation Systems*, vol. 13, no. 2, pp. 53–72, 2009.
- [8] X. Shi, Z. Chen, H. Wang, D.-Y. Yeung, W.-K. Wong, and W.-c. Woo, "Convolutional lstm network: A machine learning approach for precipitation nowcasting," *Advances in neural information processing systems*, vol. 28, 2015.
- [9] T. N. Kipf and M. Welling, "Semi-supervised classification with graph convolutional networks," *arXiv preprint arXiv:1609.02907*, 2016.
- [10] S. Hochreiter and J. Schmidhuber, "Long short-term memory," *Neural computation*, vol. 9, no. 8, pp. 1735–1780, 1997.
- [11] Z. Wu, S. Pan, G. Long, J. Jiang, X. Chang, and C. Zhang, "Connecting the dots: Multivariate time series forecasting with graph neural networks," in *Proceedings of the 26th ACM SIGKDD international conference on knowledge discovery & data mining*, 2020, pp. 753–763.
- [12] B. Yu, H. Yin, and Z. Zhu, "Spatio-temporal graph convolutional networks: A deep learning framework for traffic forecasting," *arXiv preprint arXiv:1709.04875*, 2017.
- [13] L. Bai, L. Yao, C. Li, X. Wang, and C. Wang, "Adaptive graph convolutional recurrent network for traffic forecasting," *Advances in neural information processing systems*, vol. 33, pp. 17 804–17 815, 2020.
- [14] Y. Li, R. Yu, C. Shahabi, and Y. Liu, "Diffusion convolutional recurrent neural network: Data-driven traffic forecasting," *arXiv preprint arXiv:1707.01926*, 2017.
- [15] Z. Wu, S. Pan, G. Long, J. Jiang, and C. Zhang, "Graph wavenet for deep spatial-temporal graph modeling," *arXiv preprint arXiv:1906.00121*, 2019.
- [16] J. Devlin, "Bert: Pre-training of deep bidirectional transformers for language understanding," *arXiv preprint arXiv:1810.04805*, 2018.
- [17] K. Jin, J. Wi, E. Lee, S. Kang, S. Kim, and Y. Kim, "Trafficbert: Pre-trained model with large-scale data for long-range traffic flow forecasting," *Expert Systems with Applications*, vol. 186, p. 115738, 2021.
- [18] A. Dosovitskiy, "An image is worth 16x16 words: Transformers for image recognition at scale," *arXiv preprint arXiv:2010.11929*, 2020.
- [19] K. He, X. Chen, S. Xie, Y. Li, P. Dollár, and R. Girshick, "Masked autoencoders are scalable vision learners," in *Proceedings of the IEEE/CVF conference on computer vision and pattern recognition*, 2022, pp. 16 000–16 009.
- [20] T. Zhou, P. Niu, L. Sun, R. Jin *et al.*, "One fits all: Power general time series analysis by pretrained lm," *Advances in neural information processing systems*, vol. 36, 2024.
- [21] M. Jin, Y. Zhang, W. Chen, K. Zhang, Y. Liang, B. Yang, J. Wang, S. Pan, and Q. Wen, "Position: What can large language models tell us about time series analysis," in *Forty-first International Conference on Machine Learning*, 2024.
- [22] Y. Yan, H. Wen, S. Zhong, W. Chen, H. Chen, Q. Wen, R. Zimmermann, and Y. Liang, "Urbanclip: Learning text-enhanced urban region profiling with contrastive language-image pretraining from the web," in *Proceedings of the ACM on Web Conference 2024*, 2024, pp. 4006–4017.

- [23] M. Jin, H. Y. Koh, Q. Wen, D. Zambon, C. Alippi, G. I. Webb, I. King, and S. Pan, "A survey on graph neural networks for time series: Forecasting, classification, imputation, and anomaly detection," *IEEE Transactions on Pattern Analysis and Machine Intelligence*, 2024.
- [24] Z. Jiang, "Deep learning for spatiotemporal big data: A vision on opportunities and challenges," *arXiv preprint arXiv:2310.19957*, 2023.
- [25] X. Liu, Y. Xia, Y. Liang, J. Hu, Y. Wang, L. Bai, C. Huang, Z. Liu, B. Hooi, and R. Zimmermann, "Largest: A benchmark dataset for large-scale traffic forecasting," in *Advances in Neural Information Processing Systems*, 2023.
- [26] P. Lewis, E. Perez, A. Piktus, F. Petroni, V. Karpukhin, N. Goyal, H. Küttler, M. Lewis, W.-t. Yih, T. Rocktäschel *et al.*, "Retrieval-augmented generation for knowledge-intensive nlp tasks," *Advances in Neural Information Processing Systems*, vol. 33, pp. 9459–9474, 2020.
- [27] Z. Shao, Z. Zhang, W. Wei, F. Wang, Y. Xu, X. Cao, and C. S. Jensen, "Decoupled dynamic spatial-temporal graph neural network for traffic forecasting," *Proceedings of the VLDB Endowment*, vol. 15, no. 11, pp. 2733–2746, 2022.
- [28] S. Lan, Y. Ma, W. Huang, W. Wang, H. Yang, and P. Li, "Dstagnn: Dynamic spatial-temporal aware graph neural network for traffic flow forecasting," in *International conference on machine learning*. PMLR, 2022, pp. 11 906–11 917.
- [29] Y. Lv, Y. Duan, W. Kang, Z. Li, and F.-Y. Wang, "Traffic flow prediction with big data: A deep learning approach," *Ieee transactions on intelligent transportation systems*, vol. 16, no. 2, pp. 865–873, 2014.
- [30] K. Bi, L. Xie, H. Zhang, X. Chen, X. Gu, and Q. Tian, "Accurate medium-range global weather forecasting with 3d neural networks," *Nature*, vol. 619, no. 7970, pp. 533–538, 2023.
- [31] R. Jiang, D. Yin, Z. Wang, Y. Wang, J. Deng, H. Liu, Z. Cai, J. Deng, X. Song, and R. Shibasaki, "DI-traffic: Survey and benchmark of deep learning models for urban traffic prediction," in *Proceedings of the 30th ACM international conference on information & knowledge management*, 2021, pp. 4515–4525.
- [32] Z. Zhou, J. Hu, Q. Wen, J. T. Kwok, and Y. Liang, "Multi-order wavelet derivative transform for deep time series forecasting," *arXiv preprint arXiv:2505.11781*, 2025.
- [33] J. Zhang, Y. Zheng, and D. Qi, "Deep spatio-temporal residual networks for citywide crowd flows prediction," in *Thirty-first AAAI conference on artificial intelligence*, 2017.
- [34] S. Guo, Y. Lin, N. Feng, C. Song, and H. Wan, "Attention based spatial-temporal graph convolutional networks for traffic flow forecasting," in *Proceedings of the AAAI conference on artificial intelligence*, vol. 33, no. 01, 2019, pp. 922–929.
- [35] Y. Liang, S. Ke, J. Zhang, X. Yi, and Y. Zheng, "Geomn: Multi-level attention networks for geo-sensory time series prediction," in *IJCAI*, vol. 2018, 2018, pp. 3428–3434.
- [36] C. Zheng, X. Fan, C. Wang, and J. Qi, "Gman: A graph multi-attention network for traffic prediction," in *Proceedings of the AAAI conference on artificial intelligence*, vol. 34, no. 01, 2020, pp. 1234–1241.
- [37] X. Wang, Y. Ma, Y. Wang, W. Jin, X. Wang, J. Tang, C. Jia, and J. Yu, "Traffic flow prediction via spatial temporal graph neural network," in *Proceedings of the web conference 2020*, 2020, pp. 1082–1092.
- [38] H. Liu, Z. Dong, R. Jiang, J. Deng, J. Deng, Q. Chen, and X. Song, "Spatio-temporal adaptive embedding makes vanilla transformer sota for traffic forecasting," in *Proceedings of the 32nd ACM International Conference on Information and Knowledge Management*, 2023, pp. 4125–4129.
- [39] Y. Yuan, J. Ding, J. Feng, D. Jin, and Y. Li, "Unist: a prompt-empowered universal model for urban spatio-temporal prediction," in *Proceedings of the 30th ACM SIGKDD Conference on Knowledge Discovery and Data Mining*, 2024, pp. 4095–4106.
- [40] Z. Shao, Z. Zhang, F. Wang, and Y. Xu, "Pre-training enhanced spatial-temporal graph neural network for multivariate time series forecasting," in *Proceedings of the 28th ACM SIGKDD conference on knowledge discovery and data mining*, 2022, pp. 1567–1577.
- [41] N. Kandpal, H. Deng, A. Roberts, E. Wallace, and C. Raffel, "Large language models struggle to learn long-tail knowledge," in *International Conference on Machine Learning*. PMLR, 2023, pp. 15 696–15 707.
- [42] Y. Gao, Y. Xiong, X. Gao, K. Jia, J. Pan, Y. Bi, Y. Dai, J. Sun, and H. Wang, "Retrieval-augmented generation for large language models: A survey," *arXiv preprint arXiv:2312.10997*, 2023.
- [43] A. Roberts, C. Raffel, and N. Shazeer, "How much knowledge can you pack into the parameters of a language model?" *arXiv preprint arXiv:2002.08910*, 2020.
- [44] F. Petroni, T. Rocktäschel, P. Lewis, A. Bakhtin, Y. Wu, A. H. Miller, and S. Riedel, "Language models as knowledge bases?" *Proceedings of the 2019 Conference on Empirical Methods in Natural Language Processing*, pp. 2463–2473, 2019.
- [45] K. Zhu, Y. Luo, D. Xu, R. Wang, S. Yu, S. Wang, Y. Yan, Z. Liu, X. Han, Z. Liu *et al.*, "Rageval: Scenario specific rag evaluation dataset generation framework," *arXiv preprint arXiv:2408.01262*, 2024.
- [46] G. Izacard and E. Grave, "Leveraging passage retrieval with generative models for open domain question answering," *Proceedings of the 16th Conference of the European Chapter of the Association for Computational Linguistics*, pp. 874–880, 2021.
- [47] S. Borgeaud, A. Mensch, J. Hoffmann, T. Cai, E. Rutherford, K. Millican, G. Van Den Driessche, J.-B. Lespiau, B. Damoc, A. Clark *et al.*, "Improving language models by retrieving from trillions of tokens," *International conference on machine learning*, pp. 2206–2240, 2022.
- [48] O. Ram, Y. Levine, I. Dalmedigos, D. Muhlgay, A. Shashua, K. Leyton-Brown, and Y. Shoham, "In-context retrieval-augmented language models," *Transactions of the Association for Computational Linguistics*, vol. 11, pp. 1316–1331, 2023.
- [49] W. Shi, S. Min, M. Yasunaga, M. Seo, R. James, M. Lewis, L. Zettlemoyer, and W.-t. Yih, "Replug: Retrieval-augmented black-box language models," *arXiv preprint arXiv:2301.12652*, 2023.
- [50] Z. Shao, Z. Zhang, F. Wang, W. Wei, and Y. Xu, "Spatial-temporal identity: A simple yet effective baseline for multivariate time series forecasting," in *Proceedings of the 31st ACM International Conference on Information & Knowledge Management*, 2022, pp. 4454–4458.
- [51] M. Douze, A. Guzhva, C. Deng, J. Johnson, G. Szilvasy, P.-E. Mazaré, M. Lomeli, L. Hosseini, and H. Jégou, "The faiss library," 2024.
- [52] J. Johnson, M. Douze, and H. Jégou, "Billion-scale similarity search with GPUs," *IEEE Transactions on Big Data*, vol. 7, no. 3, pp. 535–547, 2019.
- [53] C. Song, Y. Lin, S. Guo, and H. Wan, "Spatial-temporal synchronous graph convolutional networks: A new framework for spatial-temporal network data forecasting," in *Proceedings of the AAAI Conference on Artificial Intelligence*, vol. 34, no. 01, 2020, pp. 914–921.
- [54] M. Awad and R. Khanna, "Support vector regression," in *Efficient learning machines: Theories, concepts, and applications for engineers and system designers*. Springer, 2015, pp. 67–80.
- [55] C. Lea, M. D. Flynn, R. Vidal, A. Reiter, and G. D. Hager, "Temporal convolutional networks for action segmentation and detection," in *proceedings of the IEEE Conference on Computer Vision and Pattern Recognition*, 2017, pp. 156–165.
- [56] A. Vaswani, N. Shazeer, N. Parmar, J. Uszkoreit, L. Jones, A. N. Gomez, Ł. Kaiser, and I. Polosukhin, "Attention is all you need," *Advances in neural information processing systems*, vol. 30, 2017.
- [57] R. Huang, C. Huang, Y. Liu, G. Dai, and W. Kong, "Lsgcn: Long short-term traffic prediction with graph convolutional networks," in *IJCAI*, vol. 7, 2020, pp. 2355–2361.
- [58] M. Li and Z. Zhu, "Spatial-temporal fusion graph neural networks for traffic flow forecasting," in *Proceedings of the AAAI conference on artificial intelligence*, vol. 35, no. 5, 2021, pp. 4189–4196.
- [59] Z. Fang, Q. Long, G. Song, and K. Xie, "Spatial-temporal graph ode networks for traffic flow forecasting," in *Proceedings of the 27th ACM SIGKDD conference on knowledge discovery & data mining*, 2021, pp. 364–373.
- [60] Y. Chen, Y. Lv, F. Wang, and X. Zhang, "Multimodal fusion learning for traffic flow prediction," *IEEE Transactions on Intelligent Transportation Systems*, 2021.
- [61] Y. Chen, I. Segovia-Dominguez, B. Coskunuzer, and Y. Gel, "Tamp-s2gcnets: coupling time-aware multipersistence knowledge representation with spatio-supra graph convolutional networks for time-series forecasting," in *International conference on learning representations*, 2022.
- [62] X. Wang, Z. Wang, E. Wang, and Z. Sun, "Spatial-temporal knowledge distillation for lightweight network traffic anomaly detection," *Computers & Security*, vol. 137, p. 103636, 2024.
- [63] C.-C. M. Yeh, Y. Fan, X. Dai, U. S. Saini, V. Lai, P. O. Aboagye, J. Wang, H. Chen, Y. Zheng, Z. Zhuang *et al.*, "Rpmixer: Shaking up time series forecasting with random projections for large spatial-temporal data," in *Proceedings of the 30th ACM SIGKDD Conference on Knowledge Discovery and Data Mining*, 2024, pp. 3919–3930.
- [64] Y. Chen, I. Segovia, and Y. R. Gel, "Z-gcnets: Time zigzags at graph convolutional networks for time series forecasting," in *International Conference on Machine Learning*. PMLR, 2021, pp. 1684–1694.
- [65] C. Chen, K. Petty, A. Skabardonis, P. Varaiya, and Z. Jia, "Freeway performance measurement system: mining loop detector data," *Transportation research record*, vol. 1748, no. 1, pp. 96–102, 2001.

APPENDIX

We compare our model with a comprehensive set of baselines, categorized into three groups:

1) Non-Spatial Methods: **ARIMA** [5], a classical linear autoregressive moving average model for univariate time-series forecasting; **VAR** [6], a vector autoregression approach capturing linear dependencies across multiple time series; **SVR** [54], a support vector regression method leveraging kernel tricks for nonlinear time-series prediction; **LSTM** [10], a recurrent neural network architecture designed for learning long-term dependencies; **TCN** [55], a temporal convolutional network utilizing dilated causal convolutions for sequence modeling; **Transformer** [56], a self-attention-based architecture allowing parallel and long-range sequence modeling.

2) Spatial-temporal GNN Methods: **DCRNN** [14], integrating diffusion convolution with recurrent units for effective spatio-temporal modeling on graphs; **STGCN** [12], combining graph convolutions and temporal convolutions for spatio-temporal feature extraction; **ASTGCN** [34], introducing spatial and temporal attention mechanisms for dynamic feature weighting; **GWNet** [15], leveraging adaptive graph structures for flexible spatial dependency learning; **LSGCN** [57], a lightweight spatio-temporal GCN tailored for efficiency; **STSGCN** [53], utilizing spatio-temporal subgraph convolutions to capture local dependencies; **STFGNN** [58], fusing spatial and temporal features through a unified graph neural network; **STGODE** [59], employing neural ordinary differential equations to model continuous spatio-temporal dynamics; **DSTAGNN** [28], applying dynamic spatial-temporal attention for complex dependency modeling; **AGCRN** [13], using adaptive graph convolution and node-specific embeddings for personalized forecasting.

3) Other Enhanced Approaches: **Z-GCNets** [64], a zero-shot generalizable graph convolutional network for spatio-temporal prediction; **EnhanceNet** [64], an advanced spatio-temporal framework that aggregates multi-scale features for robust prediction; **TAMP** [61], leveraging temporal and spatial multi-head attention for adaptive representation learning; **STKD** [62], introducing knowledge distillation to transfer knowledge in spatio-temporal models; **RPMixer** [63], utilizing random projection layers within all-MLP mixer blocks to capture spatial-temporal dependencies.

The traffic network datasets we have used in experiments and their descriptions are as follows:

a) PEMS03/04/07/08 Dataset.: The Performance Measurement System (PeMS) datasets [65] are widely used benchmarks for traffic forecasting, maintained by the California Department of Transportation. These datasets collect real-time traffic data from sensors installed across California’s freeway system, providing multi-dimensional features including traffic flow, speed, and occupancy measurements with 5-minute temporal resolution. The adjacency matrices for these datasets are constructed based on road network distances between sensor locations. In our experiments, we follow the standard protocol of using a 70%/10%/20% split for training, validation, and testing respectively, with the temporal order preserved to ensure realistic evaluation scenarios.

b) The SD and GBA Dataset.: The LargeST benchmark [25] represents a significant advancement in large-scale

traffic forecasting datasets. This benchmark extends beyond traditional small-scale datasets by providing comprehensive large-scale traffic networks that better reflect real-world deployment scenarios. The LargeST datasets span multiple years (2017-2021) with 5-minute temporal resolution and include comprehensive metadata for spatial topology construction. For our evaluation, we adopt the data processing pipeline provided by the LargeST benchmark with a split ratio of 6:2:2, utilizing the 2019 data slice for consistent comparison with baseline methods.

A. Evaluation Metrics.

To evaluate forecasting performance, we adopt three widely-used metrics: Mean Absolute Error (MAE), Root Mean Square Error (RMSE), and Mean Absolute Percentage Error (MAPE) defined as follows. These metrics are calculated across different prediction horizons (3, 6, and 12 steps ahead) and their averages to comprehensively assess prediction accuracy at various time steps.

$$\text{MAE} = \frac{1}{|\mathcal{V}|} \sum_{(b,t,n)} |y - \hat{y}|, \quad (23)$$

$$\text{RMSE} = \sqrt{\frac{1}{|\mathcal{V}|} \sum_{(b,t,n)} (y - \hat{y})^2}, \quad (24)$$

$$\text{MAPE} = \frac{100}{|\mathcal{V}|} \sum_{(b,t,n)} \frac{|y - \hat{y}|}{y + \epsilon}, \quad (25)$$

where \mathcal{V} is the set of valid (non-missing) entries and $\epsilon = 10^{-5}$ prevents division-by-zero.

B. Training Optimization

Parameter	Value	Description
<i>Basic Training Parameters</i>		
batch_size	32	Number of samples per training batch
learning_rate	0.002	Initial learning rate for Adam optimizer
max_epochs	300	Maximum number of training epochs
weight_decay	1.0e-5	L2 regularization coefficient
eps	1.0e-8	Adam optimizer epsilon parameter
loss_function	masked_mae	Mean Absolute Error with masking
input_len	12	Length of input sequence
output_len	12	Length of prediction sequence
null_val	0.0	Null value for masking
<i>Learning Rate Scheduler</i>		
scheduler_type	MultiStepLR	Type of learning rate scheduler
milestones	[1,30,38,46,54,62,70,80]	Epochs to reduce learning rate
gamma	0.5	Learning rate reduction factor
<i>Curriculum Learning</i>		
warm_epochs	30	Number of warm-up epochs
cl_epochs	3	Curriculum learning epochs
prediction_length	12	Target prediction length
<i>Regularization</i>		
max_norm	5.0	Maximum gradient norm for clipping
train_ratio	[0.7, 0.1, 0.2]	Train/validation/test split
norm_each_channel	True	Normalize each feature channel
rescale	True	Apply data rescaling

TABLE VI: Default Training Parameters for the Experiments.

All models are implemented in PyTorch and trained on Nvidia RTX A6000 GPUs with 48GB of memory. Table VI presents the comprehensive training parameters used for RAST across all experiments. We use the Adam optimizer with a multi-step learning rate scheduler to ensure stable convergence.

Parameter	Value	Description
<i>Basic Model Parameters</i>		
num_nodes	-	Number of spatial nodes in the graph
input_dim	3	Number of input features
output_dim	1	Number of output features
<i>Model Architecture</i>		
query_dim	256	Dimension for constructed query
decoupled_layers	1	Number of decoupled encoder layers
generator_layers	3	Number of residual query fusion layers.
dropout	0.1	Dropout rate for regularization
attn_dropout	0.1	Attention dropout rate
mlp_ratio	4.0	MLP expansion ratio
output_type	full	Type of model output for ablation study
<i>Parameters for Retrieval-Augmented Mechanism</i>		
n_heads	4	Number of attention heads
retrieval_dim	128	Dimension of retrieval embeddings
top_k	5	Number of retrieved patterns
update_interval	10	Epochs between store updates
use_amp	False	Use automatic mixed precision

TABLE VII: Model Architecture Parameters for RAST.

C. Model Architecture Parameters

Table VII details the model architecture parameters for RAST. We leverage the Spatio-Temporal Retrieval Store based on the FAISS library for efficient similarity search in the retrieval store. The retrieval store utilizes GPU acceleration for index operations to maintain computational efficiency.

The theoretical foundation of RAST is grounded in information theory and memory-augmented neural networks, addressing the fundamental limitation of fixed-parameter models in capturing the full complexity of spatio-temporal patterns through external memory mechanisms. Traditional STGNNs with parameters θ can only capture information bounded by $\mathcal{I}(X; Y | \theta) \leq H(\theta)$, where $\mathcal{I}(X; Y)$ denotes the mutual information between input X and target Y , and $H(\theta)$ represents the entropy of the parameter space. Our retrieval mechanism extends this capacity by introducing external memory \mathcal{M} , enabling $\mathcal{I}(X; Y | \theta, \mathcal{M}) \leq H(\theta) + H(\mathcal{M})$. This theoretical framework allows RAST to capture more complex dependencies without increasing model parameters, providing a principled approach to enhancing model capacity through external storage.

The computational complexity of our retrieval mechanism is dominated by the similarity search operation, which leverages FAISS with inverted file index (IVF) to achieve $O(k \log M + kd)$ complexity, where k is the number of retrieved patterns, M is the memory size, and d is the embedding dimension. This represents a significant improvement over the $O(N^2)$ complexity of attention mechanisms in large graphs. The momentum-based memory update follows exponential moving average dynamics $\mathcal{M}^{(t+1)} = (1 - \alpha)\mathcal{M}^{(t)} + \alpha\mathcal{E}^{(t)}$, where α is the update rate. This formulation ensures that the memory maintains recent patterns while preserving historically significant ones, with convergence guaranteed under standard assumptions of bounded update rates and Lipschitz continuity.

Our decoupled spatial and temporal encoders employ different architectural designs optimized for their respective modalities. The temporal encoder utilizes 1D convolutions with dilation to capture multi-scale temporal patterns, while the spatial encoder employs graph convolution operations adapted to the road network topology. The multi-head attention mechanism for fusing query and retrieval embeddings uses scaled dot-product attention with temperature scaling $\tau = 0.1$ to

control attention distribution sharpness, with 16 attention heads chosen to balance representational capacity and computational efficiency. The memory management strategy implements a hybrid approach that combines temporal decay for patterns older than 50 epochs, similarity pruning for low-quality patterns below 0.3 similarity threshold, and capacity management that bounds memory size to 1000 patterns per bank to ensure computational efficiency while maintaining pattern diversity.

Despite its effectiveness, RAST faces several limitations that present opportunities for future research. The performance of our framework depends significantly on the initial memory bank construction, particularly in cold start scenarios with limited historical data, where suboptimal retrieval patterns may affect early training performance. While our retrieval mechanism effectively captures recurring patterns, it may struggle with completely novel scenarios that lack similar historical precedents in the memory bank, potentially limiting its adaptability to unprecedented events or regime changes in the data. Additionally, although computationally efficient, the retrieval operation introduces additional overhead during memory update phases, which may constrain real-time deployment in resource-limited environments. The current implementation also requires domain-specific hyperparameter tuning, particularly for similarity thresholds and memory update intervals, which may limit its plug-and-play applicability across diverse domains.

Future research directions encompass several promising avenues for enhancing retrieval-augmented spatio-temporal forecasting. Developing adaptive memory architectures that automatically adjust capacity and organization based on data complexity represents a critical advancement, potentially incorporating hierarchical memory structures and attention-based memory organization to improve pattern representation efficiency. Multi-modal integration presents another significant opportunity, where extending RAST to incorporate satellite imagery, social media data, and weather information could substantially enhance prediction accuracy in complex urban environments. The development of federated learning variants that enable privacy-preserving pattern sharing across organizations would facilitate large-scale collaborative deployment while maintaining data security.